Measurement of the useful field of view for single slices of different imaging modalities and targets

Miguel A. Lago
Ioannis Sechopoulos
François O. Bochud
Miguel P. Eckstein

Measurement of the useful field of view for single slices of different imaging modalities and targets

Miguel A. Lago,[a,*] **Ioannis Sechopoulos,**[b,c] **François O. Bochud,**[d] **and Miguel P. Eckstein**[a]

[a]University of California, Institute for Collaborative Biotechnologies, Department of Psychological and Brain Sciences, Santa Barbara, California, United States

[b]Radboud University Medical Center, Department of Radiology and Nuclear Medicine, Nijmegen, The Netherlands

[c]Dutch Expert Centre for Screening, Nijmegen, The Netherlands

[d]University Hospital and University of Lausanne, Institute of Radiation Physics, Lausanne, Switzerland

Abstract

Purpose: With three-dimensional (3-D) images displayed as stacks of 2-D images, radiologists rely more heavily on vision away from their fixation point to visually process information, guide eye movements, and detect abnormalities. Thus the ability to detect targets away from the fixation point, commonly characterized as the useful field of view (UFOV), becomes critical for these 3-D imaging modalities. We investigate how the UFOV, defined as the eccentricity, in which detection performance degrades to a given probability, varies across imaging modalities and targets.

Approach: We measure the detectability of different targets at various distances from gaze locations for single slices of liver computed tomography (CT), 2-D digital mammograms (DM), and single slices of digital breast tomosynthesis (DBT) cases. Observers with varying expertise were instructed to maintain their gaze at a point while a short display of the image was flashed and an eye tracker verified observer's steady fixation. Display times were 200 and 1000 ms for CT images and 500 ms for DM and DBT images.

Results: We find variations in the UFOV from 9 to 12 deg for liver CT to as small as 2.5 to 5 deg for calcification clusters in breast images (DM and DBT). We compare our results to those reported in the literature for lung nodules and discuss the differences across methods used to measure the UFOV, their dependence on case selection/task difficulty, viewing conditions, and observer expertise. We propose a complementary measure defined in terms of performance degradation relative to the peak foveal performance (relative-UFOV) to circumvent UFOV's variations with case selection/task difficulty.

Conclusion: Our results highlight the variations in the UFOV across imaging modalities, target types, observer expertise, and measurement methods and suggest an additional relative-UFOV measure to more thoroughly characterize the detection performance away from point of fixation.

1 Introduction

The useful field of view (UFOV) is defined as the visual area over which information can be extracted rapidly without eye or head movements.[1] The concept of UFOV, also referred to as the

---

*Address all correspondence to Miguel A. Lago, E-mail: lago@psych.ucsb.edu

functional field of view, originally pertained to scenarios with increased attentional demand. Several studies have measured the UFOV in radiology.[2–7] Traditionally, the UFOV has been defined as the distance, in which targets are detected with an 80% probability.[8,9] This value has been estimated to be a ~2.5- deg radius circle by many studies using chest radiographs and has been extensively adopted by many authors.[7,10–16] However, the UFOV size is related to the complexity of the task and image modality.[5,6,10] Some studies found that the UFOV estimate of 2.5-deg radius might be too large to be considered as an unequivocal standard.[4,17] Others have suggested considering two UFOVs, one that drives eye movements during search and another, smaller one, for recognition,[18] whereas other studies indicate a tight link between the information guiding saccades and mediating perceptual decisions.[19,20] There have been variations in how to measure the UFOV. Researchers have used the detection of peripherally presented targets or *post hoc* analyses of detection as a function of eccentricity during multiple eye movement search tasks.[5,8,21,22] Additionally, the UFOV might also be affected by the expertise of the reader, improving and increasing with training.[4,17,23,24]

With the increase in the volume of image data with newer 3-D and pseudo-3-D imaging modalities, including computed tomography (CT) and digital breast tomosynthesis (DBT), radiologists must rely more heavily in visual processing away from the point of gaze to guide their eye movements toward a region of interest.[10,13,14,25] Thus, there is renewed interest in studying the ability of observers to detect abnormalities in the visual periphery.

Here, we assess how the UFOV changes across image modalities, different targets, presentation time, and discuss its implications on search performance and model observer prediction of human performance. We report results from three studies using three different imaging modalities: single slices from hepatic CT, digital mammography, and single slices from DBT cases. The studies use a mixture of trained observers (CT) and radiologists [digital mammogram (DM) and DBT]. The studies used a steady fixation paradigm, in which observers are instructed to maintain their gaze at a given point and make a perceptual judgment about a peripherally presented target. We use real-time eye tracking to secure that observers are not making eye movements toward the targets.

2 Methods

2.1 *Stimuli*

For the first experiment, 71 healthy CT liver scans from 7 patients from the University Hospital in Lausanne, Switzerland were used as background. A signal, chosen from a real positive exam, was extracted, smoothed, and added at random locations on each trial within the liver on the healthy scans.[26] The central slice of this signal was used as the stimulus. A random slice was used for signal absent trials. We used 2560 images and 50% of the images contained an abnormality. For the second experiment, we used DM images from a subset of the Mammographic Image Analysis Society database (mini MIAS)[27] that included only calcification clusters and masses, 60 images were utilized with 50% presence of a lesion. Finally, for the DBT database, we used images collected at the Emory University School of Medicine.[28] We used the central slice of the annotated lesion as the visual stimulus. We used a random slice for signal absent trials. A total of 100 images were shown with a 50% presence of a lesion. Both DM and DBT images were annotated by experts, allowing us to have a location ground truth for the targets (calcification clusters, CALC; masses, MASS) within the image and volume, respectively. The size of the masses and calcification clusters varied from case to case. The documentation for the image database provided the lesion locations but not further information about the estimated sizes.

2.2 *Steady Fixation Signal Detection Task*

To measure human performance at different distances from the point of fixation (retinal eccentricity), we designed a steady fixation experiment. Human observers were asked to maintain fixation on one point on the screen while a cue (fiduciary cross) showed where the target might

be presented with a probability of 50%. Observers were asked to look for hypovascular hepatic tumors in one-slice CT and calcification clusters and masses on DM and one-slice DBT. All CT images were shown twice for both 200 and 1000 ms presentation times with both fixation point and attention region located within the liver. Each DM and DBT image was shown once with a single presentation time of 500 ms. Because the DM and DBT studies were conducted with radiologists (unlike the CT study), time constraints in the availability of the observers did not allow us to investigate multiple presentation times.

Given the 3-D or pseudo-3-D nature of CT and DBT modalities, we showed the slice considered as the central slice in which the target was in focus the most. Figure 1 shows the timeline for the experiments. We tested detection accuracy for target retinal eccentricities of 0, 3, 6, 9, 12, and 15 deg of visual angle for the CT images. Due to time constraints in conducting studies with radiologists, we tested fewer eccentricities for the DM and DBT images. We selected eccentricities for the masses and calcification clusters based on previous measurements with simulated signals (masses and calcifications) embedded in breast phantoms: eccentricities of 0, 2.5, and 5 deg for the calcification clusters and 0, 5, and 10 deg for the masses in both DM and DBT.

2.3 Participants

Five trained nonradiologists performed the CT experiment. The observers were seated 50 cm from a medical-grade monitor. For the DM and DBT experiments, 10 (DM) and 12 (DBT) expert radiologists were recruited at the Radiological Society of North America (RSNA) annual meeting as part of the NIH Medical Image Perception Lab. The average years of experience were 13.9 ± 11.5 for DM and 3 ± 4.2 for DBT. The average number of cases read per year was 1955 ± 2730 for DM and between 333 ± 2110 for DBT. The radiologists sat 75 cm away from a vertical medical-grade monitor following recommendations by the eye-tracker manufacturer to maximize the accuracy of eye tracking. All observers were naïve to the hypothesis of the study.

2.4 Eye Tracking

All three experiments used an EyeLink 1000 remote eye tracker during the experiments to monitor gaze location during image display. If, at any time, the tracker detected a saccade, the trial
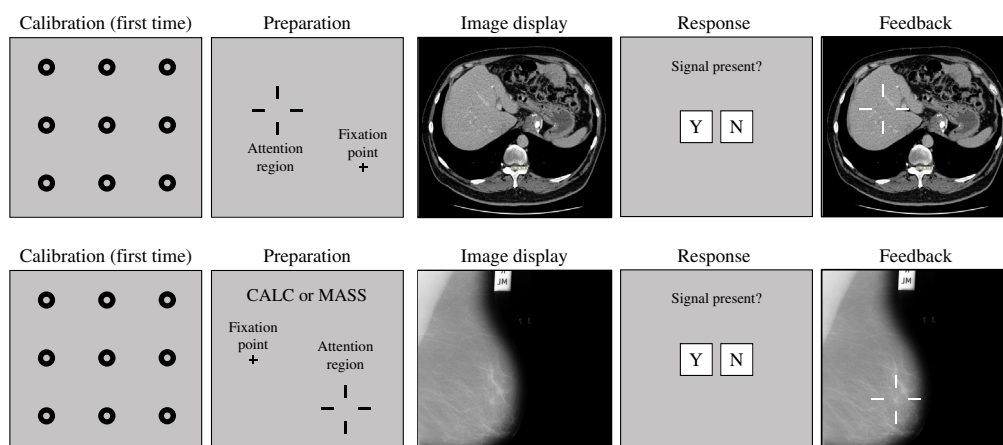

Fig. 1 Timeline of the steady fixation experiment (top: hepatic/liver CT; bottom: DM and DBT for calcification clusters, CALC, or masses, MASS). At the beginning of the experiment, observers complete a calibration routine for the eye-tracking system. The trial timeline was as follows: observers were presented with a small cross and larger fiduciary cross marks to indicate the signal location. They directed their gaze to the small cross and the test-image was displayed for a short presentation time (200 and 1000 ms for CT; 500 ms for DM and DBT). Subsequently, observers used the computer mouse to respond to the presence of the target (yes or no). Finally, observers were given feedback about whether their response was correct. Also for the DM and DBT for which there were two possible signals, observers were informed with a word (CALC or MASS) which of the two signals might be present for that trial.

was canceled and its data not accounted for the analysis. Canceled trials were 9.67% for DM and 12.4% for DBT. The percentages of canceled trials were not recorded for the CT study. Saccades were defined using the default EyeLink parameters: eye velocity higher than 35 deg/s and eye acceleration higher than 9500 deg/s^2. A calibration pattern was shown before the beginning of each session.

2.5 Performance Measures

Given the 50% prevalence of the target in the studies, we calculated the proportion correct (PC) by averaging the true positive rate (TPR, proportion of signal present trials with a positive response) and the true negative rate or $1 - $ false positive rate (FPR, proportion of signal absent trials with positive responses): PC $= [$TPR $+ (1 - FPR)]/2$. PC was calculated at each degree of eccentricity for the corresponding trials at that distance. We also report the TPR and FPR.

2.6 Definition of Useful Field of View

We define UFOV as the retinal eccentricity of the target to achieve a detection probability of 80% following the original definition.[21]

3 Results

3.1 Proportion Correct versus Retinal Eccentricity

Figure 2 shows the PC as a function of retinal eccentricity for each experiment. For the hepatic liver CT [Fig. 2(a)], the graph presents the performance for the presentation times of 200 and 1000 ms. Figures 2(b) and 2(c) show PC for calcification clusters (CALC) and masses (MASS) for DM and DBT, respectively. The results show a large variability in how PC diminishes with retinal eccentricity with reduced degradation for the hepatic CT and the mass detection in the mammograms. In contrast, PC degraded most steeply for the calcification clusters (DM and DBT).

3.2 Useful Field of View

We followed the original definition of UFOV[21] and estimated the measure for each imaging modality, presentation time (CT), and targets (DM and DBT). We obtained a range of values for the UFOV depending on the imaging modality and target to be detected. For the liver CT images, we found a UFOV of ~12-deg radius for a presentation time of 200 ms and a ~15-deg
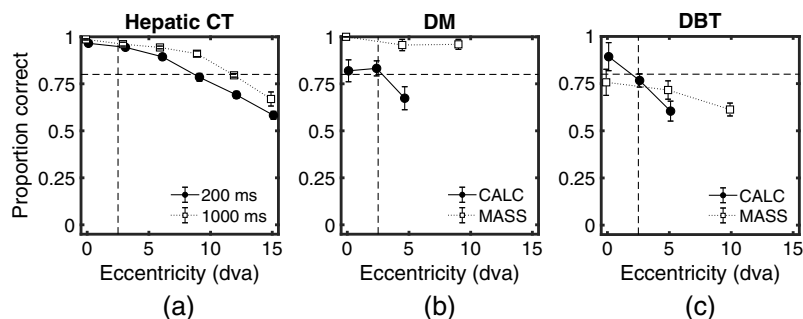

Fig. 2 PC detecting the signal for the three different experiments. (a) Hepatic CT for presentation times of 200 and 1000 ms. (b) DM for a presentation time of 500 ms for calcification clusters (CALC) and masses (MASS). (c) DBT for a presentation time of 500 ms for CALC and MASS. Vertical and horizontal dashed lines at 2.5 deg and 0.8 PC were drawn as a reference for the currently accepted UFOV radius and its expected PC. Error bars are the standard error of the mean across observers.

radius for 1000 ms. For the mammograms, calcifications UFOV was closer to ∼3- deg radius. For the masses, the PC was higher than 0.8 for all tested conditions, thus we can conclude that the UFOV is larger than 10 deg. For the DBT images, the estimated UFOV for the calcifications is, again, ∼3- deg radius. For masses in single-slice DBT images, only at 0 deg did the PC reach a nonsignificantly different from 0.8, whereas at 5 and 10 deg PC was significantly ($p < 0.05$) lower than 0.8. This suggests a UFOV that is <5 deg. Additionally, for the masses in the DBT images, there was a steeper degradation than with the mammograms.

3.3 Relative Useful Field of View

One limitation of the UFOV is that it can be influenced by the overall difficulty of the cases or details of the experimental methods (e.g., time of presentation). To assess the degradation in performance at the visual periphery relative to the fovea independent of the case or task difficulty, we defined a complementary measure, relative useful field of view (RUFOV). We defined the RUFOV as the distance to the fovea (retinal eccentricity), in which detection probability degraded by 15% of the peak foveal performance (e.g., 15% of 80% peak performance would correspond to 12% decrement detection probability). We used linear interpolation between neighboring data points to estimate the RUFOV. For the hepatic CT experiment, the RUFOV was 8.15 deg for 200 ms presentation time and 10.88 deg for 1000 ms presentation time. For the DM experiment, the RUFOV was 4.22 deg for calcifications and >10 deg for masses. For the DBT experiment, the RUFOV was 2.62 deg for calcifications and 8.52 deg for masses.

3.4 Analysis of Hit Rate and False Positive Rate

To further analyze the results, we partitioned performance into TPR and FPR. Figure 3 shows the results for each imaging modality: hepatic CT (presentation time of 200 and 1000 ms), DM and DBT (target type CALC and MASS). In general, all results show that PC degradation with retinal eccentricity (Fig. 2) is related mainly to reductions in TPR. However, for the hepatic CT, the results also show a significant increase in FPRs with retinal eccentricity: the mean FPR for close eccentricities (0, 3, and 6 deg) was significantly different from that for larger eccentricities (9, 12, and 15 deg), $p < 0.05$. No significant increase in FPR was found for the mammograms nor the DBT. Furthermore, for the DBT images, we found a significant decrease in FPR for the masses but less steep than the decrease in TPR.
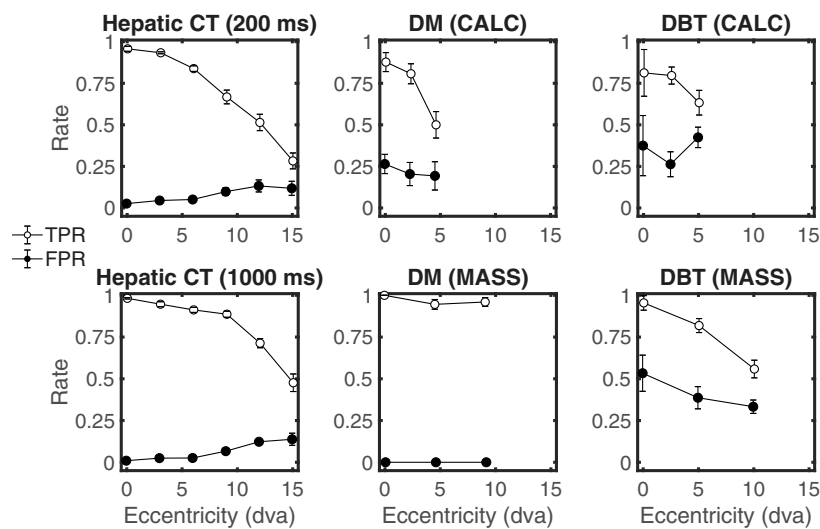

Fig. 3 TPR and FPR as a function of target retinal eccentricity (degrees visual angle) for hepatic liver CT, DM, and DBT studies. Error bars are the standard error of the mean across observers.

4 Discussion

Our goal was to measure perceptual performance in detecting clinically important visual features in the visual periphery for different imaging modalities, targets, and presentations times to assess the size of the UFOV. Our findings corroborate the previously indicated idea that the UFOV can vary dramatically with the difficulty of the task.[6,10]

Here we show that the UFOV varies abruptly across imaging modalities and target type: from 2.5-deg radius (calcifications in DM in DBT) to 12- to 15-deg (hepatic CT). Similarly, using the standard UFOV value of 2.5-deg radius leads to very different detection performances across modalities and targets (Fig. 2). Also even the presentation time (CT images) will improve detection performance across all eccentricities and moderately influence the UFOV (from 12 deg to 15 deg for the CT images).

A possible confounding variable in our comparison across studies is that the hepatic CT evaluation was performed by trained nonradiologists, whereas DM and DBT studies were conducted by radiologists. The level of expertise across observers could be considered a confounding variable that could account for the different results across modalities. However, previous studies have shown that expertise increases the visibility of the target in the periphery, thus increasing the UFOV.[4,17,23,24] It is expected that the naïve observers who viewed the CT images have a smaller UFOV than radiologists. Thus, had we used radiologists in the CT study, it is likely that we would have obtained even larger differences in UFOVs across CT versus DM/DBT.

Another seemingly puzzling finding is the difference in UFOV results for the detection of masses in the DM (>10 deg) and DBT (<5 deg) images. There are various possible explanations. The definition of the UFOV depends both on the degradation of performance at the visual periphery and case difficulty. For DM images, masses were more detectable at both fovea and periphery than calcification clusters and rarely missed. On the contrary, for DBT images, masses were less detectable at the fovea than calcification clusters. This result could be due to variations in case difficulty or simply the fact that the typical dose for a single slice in DBT is only a fraction of the dose for a DM image. Thus, there is additional noise (lower SNR) in a single-slice DBT image than a DM image. Also, radiologists had more years of experience reading DM when compared to the DBT images. This difference simply reflects the fact that DBT technology is newer. Thus, the higher performance for masses in DM versus single slices of DBTs might also be due to higher expertise with DMs. To circumvent the effects of overall task difficulty when comparing across modalities, we defined a complementary metric (RUFOV) that measured the degradation in performance relative to the peak detection at the fovea (see Sec. 3.3). The RUFOV measures resulted in more similar values across DM and DBT. For both modalities, calcification detection degraded more abruptly in the periphery than the detection of masses. This result is consistent with the common opinion from practicing radiologists that the UFOV for masses is typically larger than for calcification clusters.

Our fixation study with DBTs utilized the central slice of the DBT rather than the actual volume. Our UFOV measurements do not apply to situations in which the radiologist is scrolling through the slices of the DBT images. Instead, the measurements are likely applicable to clinical scenarios, in which radiologists engage in scanning behavior and with no scrolling. During scanning, the radiologist scrutinizes a single slice and searches different regions through eye movements. At each fixation, the observers process information in the visual periphery to guide the next eye movement.[12,29] The visibility of the targets in the visual periphery is critical to guide the eye movements toward likely target locations.[19,20,29–31] Previous studies have shown that overall detection performance improves for simulated masses in 3-D volumes[14] as well as real masses in DBT images.[32] Thus, it is likely that the foveal and peripheral performance would increase during active multiple slice scrolling and UFOV measurements would increase for multiple slice DBT images. However, it is not clear whether the RUFOV would change for single versus multiple slice DBTs. Future studies should assess how the current results relate to the UFOV and RUFOV while radiologists/observers are fixated at a point and drill/scroll through the volume slices.

An additional interesting finding is an increase in the FPR with retinal eccentricity for hepatic CTs while there is a reduction for DBT images. There is a strong possibility that this result might

be related to differences across trained nonradiologists (CT) and radiologists (DBT) but future studies should further evaluate this hypothesis.

Table 1 compares our results to those existing in the literature. For each study, the table summarizes the method used to measure the UFOV, the participant population, and reported years of experience, estimated UFOV and our estimate of RUFOV extracted from the reported data (when possible). Typical reported values for the UFOVs for lung nodules in radiography images vary from 3 to 5 deg. For lung nodules in multislice CT images, the reported UFOV varies from 2.5 deg for smaller targets to 7.5 deg for larger targets. Table 1 also shows the reported UFOV for our study. When possible we also estimated the RUFOV for the previous studies with values varying from 1 deg for the detection of lung nodules in radiographs to 7.5 deg for large nodules in multislice CT.

Importantly, we emphasize that there are large variations in the methods used to measure the UFOV across studies (see Table 1). These differences across methods might influence the results. Carmody et al.[21] and Ebner et al.[5] used a method similar to the present paper: observers maintained their gaze at a fixed point and detect a target that might appear at different distances from fixation. Rubin et al.[22] used a method, in which observers freely search with eye movements through images and then assess the distance from the fovea, in which 99.8% of the targets are

Table 1 Research reporting the UFOV in medical images and estimated RUFOV.

Author	Target and modality	Observers	Methodology	UFOV definition	RUFOV
Carmody et al.[21]	Lung nodules (radiography)	1 radiologist, 1 experienced reader	Steady fixation 360 ms	Reduction of foveal PC by 50% at 5 deg	~1.5 deg
Kundel et al.[7]	Lung nodules (radiography)	1 radiologist, 1 experienced reader	Search % of total image nodules detected within an increasing visual field	80% PC at 3 to 4 deg	N/A
Rubin et al.[22]	Lung nodules (CT)	13 radiologists 8.6 ± 8.0 years of experience	Search	99.8% detected nodules at 2.6 deg	N/A
Ebner et al.[5]	Lung nodules (CT)	6 radiologists 6 to 12 years of experience	Steady fixation 13 s drilling video 1 of 32 locations	80% PC small target < 2.5 deg	Small target: ~4 deg
				80% PC large target 5 to 7.5 deg	Large target: ~7.5 deg
This paper	Hepatic (single-slice CT)	5 nonradiologists trained observers	Steady fixation 200 and 1000 ms presentation cued single location	80% PC 200 ms: 9 deg	200 ms: 8.15 deg
				80% PC 1000 ms: 12 deg	1000 ms: 10.88 deg
	Breast CALC (DM)	10 radiologists 13.9 ± 11.5 years of experience	Steady fixation 500 ms presentation cued single location	80% PC 2.5 to 5 deg	4.22 deg > 10 deg
	Breast MASS (DM)			80% PC > 10 deg	
	Breast CALC (single-slice DBT)	12 radiologists 3 ± 4.2 years of experience		80% PC 2 to 3 deg	2.62 deg
	Breast MASS (single-slice DBT)			80% PC < 5 deg	8.52 deg

detected across all trials/images. Kundel et al.[7,8] used a hybrid method relying on eye movement measurements during a search task and estimates the probability of target detection within a field of view using the peripheral measurements of Carmody et al.[21] The UFOV measurement method relying on eye movement is more representative of the clinical situation in assessing the ability to successfully detect the target during the search process. Yet, its limitation is that it does not isolate the perceptual processing corresponding from a single fixation and peripheral location of the target. Presumably, visual processing from various fixations with different target retinal eccentricities can potentially contribute to the detection of the target,[29] not just the fixation with the target within the empirically estimated UFOV. The advantage of the steady fixation method is that it isolates the contributions to target detection of a single fixation and a well-controlled target retinal eccentricity. Its main drawback is that it is not embedded in the search process and, therefore, less clinically realistic.

One additional difference between the Ebner et al. and Carmody et al. method and the one in this paper is that the former did not provide a visual cue indicating a single target location but rather utilized 32 possible locations. Spatial uncertainty about the target location is known to degrade detection performance[33–35] so our values for the UFOV would likely be even smaller if we utilized a paradigm with multiple locations as in Ebner et al. Furthermore, Ebner et al.'s experiment was a 13-s video drilling through a 5-cm volume, which might have also influenced the target detection rates.

Another fundamental limitation in comparing the estimated UFOVs is that studies use different detection probabilities to define the UFOV (see column 5 in Table 1).

5 Conclusion

We have shown how the UFOV can be very different when we compare different image modalities and targets. In general, single-slice hepatic CTs led to the largest UFOVs and calcification clusters in mammograms and single-slice DBT images to UFOVs that are comparable to that of the smallest nodules in lung planar x-rays or CT images. We highlight how the methods used to measure UFOVs should be considered when comparing results across studies. We also propose a relative UFOV as a complementary measure that does not depend on task difficulty. Together, the results confirm the notion that the standard UFOV of 2.5-deg radius should not be taken as a one-size-fits-all measure. The imaging modality, task, target, as well as measurement method, and expertise will influence the estimate of the UFOV. To fully evaluate CT and DBT, future studies should compare the single-slice measurements in this study with multislice UFOV measurements. The comparison of our results with classic studies reveals that there is a need to further understand the relationship among the various methods to measure UFOV and also to develop methodology standards to allow for effective comparisons across studies.

Disclosures

This research was performed under an IRB protocol for human data (12-16-0806) approved by the University of California, Santa Barbara. The authors declare no conflicts of interest.

Acknowledgments

References

1. R. Sekuler and K. Ball, "Visual localization: age and practice," *J. Opt. Soc. Am. A* **3**(6), 864–867 (1986).

2. E. A. Krupinski et al., "Eye-movement study and human performance using telepathology virtual slides. Implications for medical education and differences with experience," *Hum. Pathol.* **37**(12), 1543–1556 (2006).
3. L. H. Williams and T. Drew, "Distraction in diagnostic radiology: how is search through volumetric medical images affected by interruptions?" *Cognit. Res. Princ. Implic.* **2**(1), 12 (2017).
4. A. H. Young and J. Hulleman, "Eye movements reveal how task difficulty moulds visual search," *J. Exp. Psychol.* **39**(1), 168–190 (2013).
5. L. Ebner et al., "Variations in the functional visual field for detection of lung nodules on chest computed tomography: impact of nodule size, distance, and local lung complexity," *Med. Phys.* **44**(7), 3483–3490 (2017).
6. C.-C. Wu and J. M. Wolfe, "Eye movements in medical image perception: a selective review of past, present and future," *Vision* **3**(2), 32 (2019).
7. H. L. Kundel, C. F. Nodine, and E. A. Krupinski, "Searching for lung nodules. Visual dwell indicates locations of false-positive and false-negative decisions," *Invest. Radiol.* **24**(6), 472–478 (1989).
8. H. L. Kundel et al., "Searching for lung nodules a comparison of human performance with random and systematic scanning models," *Invest. Radiol.* **22**(5), 417–422 (1987).
9. H. L. Kundel, "Perception errors in chest radiography," *Semin. Respir. Med.* **10**, 203–210 (1989).
10. L. H. Williams and T. Drew, "What do we know about volumetric medical image interpretation?: A review of the basic science and medical image perception literatures," *Cognit. Res. Princ. Implic.* **4**(1), 21 (2019).
11. A. G. Gale et al., "Is airport baggage inspection just another medical image?" *Proc. SPIE* **3981**, 184–192 (2000).
12. J. Najemnik and W. S. Geisler, "Eye movement statistics in humans are consistent with an optimal search strategy," *J. Vision* **8**(3), 4 (2008).
13. T. Drew et al., "Scanners and drillers: characterizing expert visual search through volumetric images," *J. Vision* **13**(10), 3 (2013).
14. M. A. Lago et al., "Interactions of lesion detectability and size across single-slice DBT and 3D DBT," *Proc. SPIE* **10577**, 105770X (2018).
15. A. Aizenman et al., "Comparing search patterns in digital breast tomosynthesis and full-field digital mammography: an eye tracking study," *J. Med. Imaging* **4**(4), 045501 (2017).
16. C. F. Nodine et al., "Time course of perception and decision making during mammographic interpretation," *Am. J. Roentgenol.* **179**(4), 917–923 (2002).
17. T. Drew, S. E. P. Boettcher, and J. M. Wolfe, "One visual search, many memory searches: an eye-tracking investigation of hybrid search," *J. Vision* **17**(11), 5 (2017).
18. J. Hulleman and C. N. Olivers, "The impending demise of the item in visual search," *Behav. Brain Sci.* **40**, e132 (2017).
19. B. R. Beutter, M. P. Eckstein, and L. S. Stone, "Saccadic and perceptual performance in visual search tasks. I. Contrast detection and discrimination," *J. Opt. Soc. Am. A* **20**(7), 1341–1355 (2003).
20. M. P. Eckstein et al., "Similar neural representations of the target for saccades and perception during search," *J. Neurosci.* **27**(6), 1266–1270 (2007).
21. D. P. Carmody, C. F. Nodine, and H. L. Kundel, "An analysis of perceptual and cognitive factors in radiographic interpretation," *Perception* **9**(3), 339–344 (1980).
22. G. D. Rubin et al., "Characterizing search, recognition, and decision in the detection of lung nodules on CT scans: elucidation with eye tracking," *Radiology* **274**(1), 276–286 (2015).
23. K. K. Ball et al., "Age and visual search: expanding the useful field of view," *J. Opt. Soc. Am. A* **5**(12), 2210–2219 (1988).
24. S. L. Willis et al., "Long-term effects of cognitive training on everyday functional outcomes in older adults," *JAMA* **296**(23), 2805–2814 (2006).
25. M. P. Eckstein, M. A. Lago, and C. K. Abbey, "The role of extra-foveal processing in 3D imaging," *Proc. SPIE* **10136**, 101360E (2017).
26. I. Diaz et al., "Measurements of the detectability of hepatic hypovascular metastases as a function of retinal eccentricity in CT images," *Proc. SPIE* **8318**, 83180J (2012).

27. "The mini-MIAS database of mammograms," http://peipa.essex.ac.uk/info/mias.html (accessed 23 September 2019).

28. G. A. Agasthya et al., "Reduction in digital breast tomosynthesis interpretation time by slabbing of the reconstructed slices," in *Eur. Cong. Radiol.*, Vienna (2016).

29. C. J. H. Ludwig, J. R. Davies, and M. P. Eckstein, "Foveal analysis and peripheral selection during active visual sampling," *Proc. Natl. Acad. Sci. U. S. A.* **111**(2), E291–E299 (2014).

30. P. Viviani and R. G. Swensson, "Saccadic eye movements to peripherally discriminated visual targets," *J. Exp. Psychol.* **8**(1), 113–126 (1982).

31. J. M. Findlay, "Saccade target selection during visual search," *Vision Res.* **37**(5), 617–631 (1997).

32. M. Noroozian et al., "Digital breast tomosynthesis is comparable to mammographic spot views for mass characterization," *Radiology* **262**(1), 61–68 (2012).

33. A. E. Burgess and H. Ghandeharian, "Visual signal detection. II. Signal-location identification," *J. Opt. Soc. Am. A* **1**(8), 906–910 (1984).

34. M. P. Eckstein and J. S. Whiting, "Visual signal detection in structured backgrounds. I. Effect of number of possible spatial locations and signal contrast," *J. Opt. Soc. Am. A* **13**(9), 1777–1787 (1996).

35. F. O. Bochud, C. K. Abbey, and M. P. Eckstein, "Search for lesions in mammograms: statistical characterization of observer responses," *Med. Phys.* **31**(1), 24–36 (2004).

Miguel A. Lago is a postdoctoral scholar in the Department of Psychological and Brain Sciences at the University of California Santa Barbara. His background is in computer engineering and his research studies how visual search in 3-D medical image modalities affect observer performance and efficiency in radiology.

Ioannis Sechopoulos is a medical physicist and an associate professor in the Department of Radiology and Nuclear Medicine, Radboud University Medical Center, Nijmegen, where he is the director of the Advanced X-ray Tomographic Imaging (AXTI) Lab. He also conducts research on breast cancer screening at the Dutch Expert Centre for Screening.

François O. Bochud has worked as a medical physicist for more than 20 years. He is the director of the Institute of Radiation Physics, University Hospital and University of Lausanne. His research involves medical imaging including, dosimetry, texture analysis, and model observers dedicated to the detection task, especially in mammography and more recently in CT.

Miguel P. Eckstein is a professor in the Department of Psychological and Brain Sciences and affiliate faculty in the Department of Electrical and Computer Engineering at the University of California Santa Barbara. His research uses a variety of tools including behavioral psychophysics, eye tracking, electro-encephalography, functional magnetic resonance imaging, and computational modeling to study how humans see. His findings are applied to problems in medical imaging, computer vision, and interactions between robots/computer systems and humans.